Environmental Research 163 (2018) 208–216

Contents lists available at ScienceDirect

Environmental Research

journal homepage: www.elsevier.com/locate/envres

# The human skin as a sub-THz receiver – Does 5G pose a danger to it or not?

Noa Betzalel[a], Paul Ben Ishai[a,b], Yuri Feldman[a,*]

[a] Department of Applied Physics, The Rachel and Selim Benin School of Engineering and Computer Science, The Hebrew University of Jerusalem, Edmond J. Safra Campus, Jerusalem 91904, Israel

[b] Department of Physics, Ariel University, Ariel 40700, Israel

ARTICLE INFO

*Keywords:*
5G
Helical antenna
Human skin, Sub-Terahertz (sub-THz)
Specific Absorption Rate (SAR)
Sweat duct

ABSTRACT

In the interaction of microwave radiation and human beings, the skin is traditionally considered as just an absorbing sponge stratum filled with water. In previous works, we showed that this view is flawed when we demonstrated that the coiled portion of the sweat duct in upper skin layer is regarded as a helical antenna in the sub-THz band. Experimentally we showed that the reflectance of the human skin in the sub-THz region depends on the intensity of perspiration, i.e. sweat duct's conductivity, and correlates with levels of human stress (physical, mental and emotional). Later on, we detected circular dichroism in the reflectance from the skin, a signature of the axial mode of a helical antenna. The full ramifications of what these findings represent in the human condition are still unclear. We also revealed correlation of electrocardiography (ECG) parameters to the sub-THz reflection coefficient of human skin. In a recent work, we developed a unique simulation tool of human skin, taking into account the skin multi-layer structure together with the helical segment of the sweat duct embedded in it. The presence of the sweat duct led to a high specific absorption rate (SAR) of the skin in extremely high frequency band. In this paper, we summarize the physical evidence for this phenomenon and consider its implication for the future exploitation of the electromagnetic spectrum by wireless communication. Starting from July 2016 the US Federal Communications Commission (FCC) has adopted new rules for wireless broadband operations above 24 GHz (5 G). This trend of exploitation is predicted to expand to higher frequencies in the sub-THz region. One must consider the implications of human immersion in the electromagnetic noise, caused by devices working at the very same frequencies as those, to which the sweat duct (as a helical antenna) is most attuned. We are raising a warning flag against the unrestricted use of sub-THz technologies for communication, before the possible consequences for public health are explored.

## 1. Introduction

The world is galloping towards a bright new future, or at least so industry would like us to think. The advent of 5 G promises unforetold connectivity and unparalleled integration with the virtual world (Agiwal et al., 2016). Technology will interact with almost every aspect of our daily lives (Boccardi et al., 2014), as well as expose us to rich and varied data streaming on our cellular and Wi-Fi devices. While all of this may be true it comes with a price tag. To afford such heavy data traffic we must accept an expansion in data channels (Ben Ishai et al., 2016), something that is not possible in the currently used frequency channels, and an attendant explosion in base stations (Ge et al., 2016). This is the rational to move to 5 G, a FCC standard, which will start at 28 GHz (FCC Report 16–89), soon utilize frequencies up to 60 GHz and may eventually reach the sub - Terahertz range (FCC 50–50 Report).

Industry has assumed that there will be no health risks from this advance (T. Wu et al., 2015a, 2015b) and consequently it has based its planning on the recommendations of the International Commission on Non-Ionizing Radiation Protection (ICNIRP), published in 1998 (Guidelines for limiting exposure to time-varying electric, magnetic, and electromagnetic fields (up to 300 GHz). International Commission on Non-Ionizing Radiation Protection," 1998). This recommendation limits exposure in the 5 G range to a power density of 10 $W/m^2$ for the general public and to 50 $W/m^2$ for occupational exposure ("Guidelines for limiting exposure to time-varying electric, magnetic, and electromagnetic fields (up to 300 GHz). International Commission on Non-Ionizing Radiation Protection," 1998).

However, in recent years concerns have surfaced about possible non-thermal biological effects, and ensuing health issues, arising from cellular electromagnetic radiation (Adams et al., 2014; Blank and Goodman, 2009; Darbandi et al., 2017; Hardell and Sage, 2008; Liu et al., 2013; Panagopoulos, 2017; Sage and Carpenter, 2009; Terzi et al., 2016). These should raise a red flag for the implementation of the 5 G standard. One reason being that the modality of our interaction

* Corresponding author.
*E-mail address:* yurif@mail.huji.ac.il (Y. Feldman).

https://doi.org/10.1016/j.envres.2018.01.032
Received 2 September 2017; Received in revised form 18 December 2017; Accepted 23 January 2018

with EM waves changes from direct absorption to a more complex form. This is because the wavelengths involved approach the dimensions of the skin structures, leading to standing wave effects between strata. Furthermore, in 2008, we pioneered the hypothesis that because of the coiled nature of sweat ducts in human skin, they could function as an array of low-Q helical antennas at the sub-THz frequencies (Feldman et al., 2008, 2009). In other words, there would be a set of frequencies, ideally suited to be absorbed by our skin. Worryingly, there is some evidence for non-thermal biological effects in this frequency range (Zhadobov et al., 2011; Le Dréan et al., 2013; Habauzit et al., 2014; Mahamoud et al., 2016).

In this work we will outline the basic scientific background for this concept and the physical evidence confirming the phenomena. We will then explore the implications for the simulation of EM interaction with the skin and introduce a realistic skin model. Finally, we will calculate the expected Specific Absorption Rate (SAR) of the skin in the frequency range covered by the 5G standard.

## 2. Scientific background

Studies of the morphology of the skin by optical coherence tomography (OCT) revealed that the tips of the sweat ducts that expel the sweat from the gland to the pore at the surface of the skin have a helical structure (see Fig. 1) (Serup and Trier-Mork, 2007). This, together with the fact that the dielectric permittivity of the dermis is higher than that of the epidermis (Gabriel et al., 1996), brings forward the assumption that as electromagnetic entities, the sweat ducts could be regarded as imperfect helical antennas with both end-fire and normal modes.

By applying basic antenna theory (Kraus and Marhefka, 2001) to the typical duct dimensions, and using the known dielectric and conductivity characteristics of the skin tissue (Feldman et al., 2009), the bandwidth was found to be in the sub-THz frequency range (see Fig. 2).

Since electric conductivity is necessary for operation of any electromagnetic (EM) device, it was proposed that the *ac* electric current "activated" in the "duct antenna" would be due to the diffusion of protons via hopping through distributed H-bond networks (see Fig. 3), known to exist in biological structures (Feldman et al., 2009; Hayut et al., 2013). In bulk water, at 100 GHz, *ac* conductivity was measured and found to be ~100 S/m (Ellison et al., 1996). There is evidence that in the vicinity of a lipid/water interface, such as that along the inner surface of the sweat duct, water is well-structured (Kim et al., 2006). In such layers adjacent to the epithelia cells of the sweat duct, an increase in the proton diffusion rate by a factor of 100 (Brändén et al., 2006) in comparison to that in bulk water, was found by fluorescence spectroscopy. The skin contains between 2 and 5 million sweat ducts (Nishiyama et al., 2001) spread over the body, with differing distribution densities depending on body zone.

Furthermore sweat ducts constitute an active system, working according to a number of different stimuli (physiological, mental, emotional, or gustatory), not only due to thermoregulation (Guyton, 1990). Consequently, one would expect that the sub-THz spectra of the reflection coefficient (R) are also functions of skin morphology, the distribution of perspiration activity over the skin surface and the stimuli causing the sweating. The supposition pertaining to morphology and activity was substantiated by a series of experiments and computer simulations that showed that the spectral response of the ducts indeed coincides with the prediction of antenna theory (Feldman et al., 2009; Hayut et al., 2013).

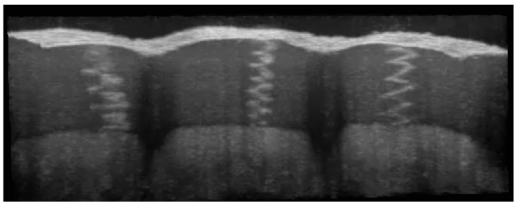

**Fig. 1.** OCT imaging of the sweat ducts in upper epidermis of the human fingertip in vivo (Lademann et al., 2007).

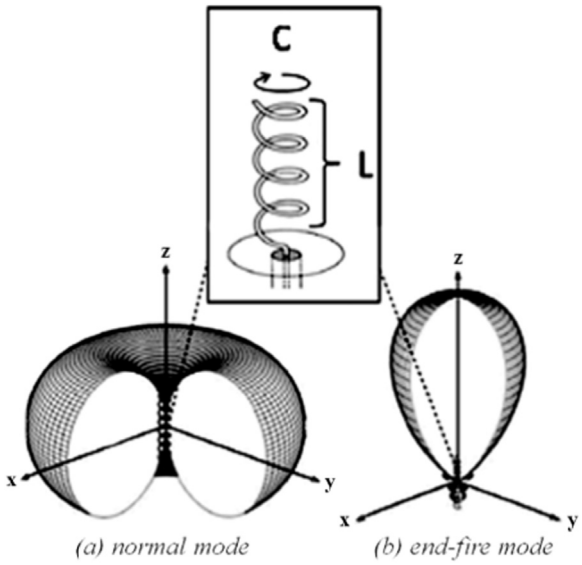


**Fig. 2.** Three-dimensional power patterns for the helical antenna (a) normal mode and (b) axial (also called end-fire) mode (Kraus and Marhefka, 2001); the characteristic frequency of the modes depends on the dimensions C and L respectively. $f \sim \frac{1}{C} \times$ 400 GHz and $f \sim \frac{1}{L} \times$ 100 GHz.

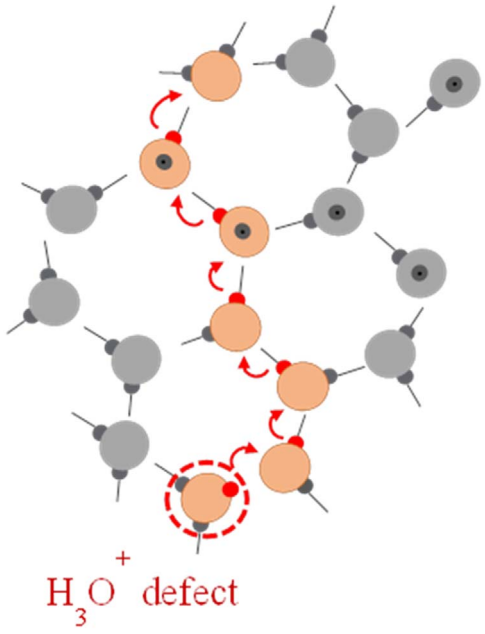


**Fig. 3.** Schematic presentation of the proton hopping (Ben Ishai et al., 2015; Popov et al., 2016) through a distributed H-bond network.

## 3. Experimental methods

The results obtained from the simulation work were verified in series of in vivo experiments conducted on a number of subjects in the W-band (75–110 GHz). It was shown that the reflection coefficient of their skin strongly depends on the physiological stress of the subject (Feldman et al., 2009, 2008). In the experiments, the palm was held steady by a stand that was placed at fixed distance from the horn antenna connected to the input of the Vector Network Analyzer (VNA). The measurements were carried out using 13 subjects, both male and

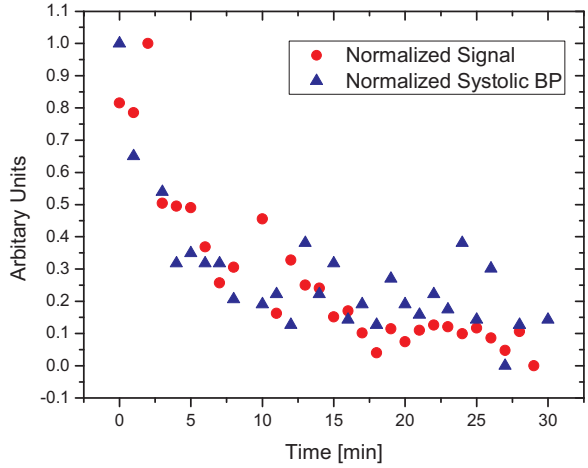


**Fig. 4.** The relative signal intensity (75–110 GHz) of the subject's palm, following 20 min of the intense physical activity (Feldman et al., 2008) and the normalized systolic blood pressure, measured for the same subject during the same experiment.

female, all were in the age group 20–30 and had given their informed consent. The experiments were carried out with the permission of the Ethics Committee of the Hebrew University of Jerusalem. Every experimental run included both the measurement of skin reflectance and simultaneous recordings of the pulse rate, the systolic blood pressure, and the skin temperature. The subjects jogged for 20 min, and afterward a series of 30 measurements were conducted at 1 min intervals. These signals were compared to those of the same person measured when seated calm before the exercise. The results of the typical experimental run are presented in Fig. 4. The skin reflectance is presented in terms of the relative signal intensity averaged over frequency interval, namely as

$$<W(t)>_f = \frac{1}{f_2 - f_1}\int_{f_1}^{f_2} \frac{(|U_{subject}(f,t)|^2}{|U_{reference}(f,t)|^2} df \quad (1)$$

Where $U_{subject}(f, t)$ is the signal reflected from the subject after his/her physical activity, $U_{reference}(f, t)$ is the signal taken from the same subject before engaging in physical activity. The frequency range was between $f_1 = 75$ GHz and $f_2 = 110$ GHz. in this particular set of the experiments.

After physical activity an exponential-like decay can be observed in signal intensity (Fig. 4), and it correlates well with the relaxation rate of the subject's systolic blood pressure (Feldman et al., 2009, 2008). Care was taken to eliminate blood perfusion in the skin layer as the origin of any change in the reflection coefficient by artificially varying perfusion using an armband pressure cuff. This had no effect on the measured signal in the W-band (Feldman et al., 2009, 2008). As a further measure, sweat gland activity on the palm of the hand was stopped by the application of a cream containing snake venom-like synthetic tripeptide acting as an antagonist of the postsynaptic muscular nicotinic acetylcholine membrane's receptor (mnAChR) (Feldman et al., 2008). The subsequent signal was greatly reduced, pointing to the sweat duct as the origin of the observed response.

Sweat glands are directly controlled by the Sympathetic Nerve System (SNS) (Ohhashi et al., 1998). Consequently, stress, emotion, fear, pain, anxiety and disease can induce sweating (Eisenach et al., 2005; Ziegler and Heidl, 2008). This provokes the question whether very gentle stimulation of the SNS, e.g., mental activity rather than intense physical activity, can elicit a detectable electromagnetic response of the skin. In order to answer this, one must correlate the EM response to recognized triggers of mental stress (Safrai et al., 2012). There are several common ways to evoke mental stress, such as the Stroop effect (Stroop, 1935), speaking in front of an audience and performing mental arithmetic calculations (Kirschbaum et al., 1993). We chose to exploit the Stroop effect during which a person is subjected to confounding semantic and visual inputs. For example, the subject is requested to name the color of the fonts used to write the name of a different color, e.g., the word “blue” is written in red. Such an experiment is also called a color word test (CWT). This test was chosen since its duration is longer than most other mental tests (about 15 min), even though it induces only mild stress.

Stress can be monitored in a number of ways, including tracing the pulse rate, blood pressure, electrocardiogram, and other physiological parameters (Cacioppo et al., 2007). However, the most popular stress-detection method is based on the Galvanic Skin Response (GSR). Measuring the GSR is a standard approach for tracking changes in the SNS of a human subjected to psychological stress (Hubbard et al., 1992; Muter et al., 1993). The results of our recent study (Safrai et al., 2012) clearly indicate that the reflection coefficient of the human hand in both W (75–110 GHz) and D (110–170 GHz) bands is correlated to universally accepted indicators of mental stress. The signals averaged over both frequency bands had correlations ranging from 0.74 to 0.93 for common indicators of stress, i.e. blood pressure and pulse rate. Particularly, the correlation between the GSR signal and $<W>_f$ in the D band reaches 0.82 (Safrai et al., 2012).

Another intriguing correlation is raised by use of parameters derived from the electrocardiogram (ECG). The ECG trace highly informative regarding myocardial health and function. As stress changes heart activity, much data may be gathered regarding the intensity of the stress from the ECG trace and the parameters derived therein. In particular the ST elevation parameter of the trace is an important element in diagnosing heart disease (Muter et al., 1993). Recently we showed a strong correlation between ST elevation and the reflection coefficient in the D band (Safrai et al., 2014). Despite this correlation with physiological and mental stresses (Feldman et al., 2009, 2008; Safrai et al., 2012), the link between the electromagnetic reflection properties of the skin and the helical structure of the sweat duct remained questionable. The key to identifying such a necessary link can be found in an important property of the sweat ducts' helical structure-homochirality. If the majority of sweat ducts exhibit a right-handed turn, then this homogeneity will mean that an electromagnetic wave reflected from them will exhibit predominantly right-handed circular polarization (see Fig. 5).

The predominance of right-handed over left-handed polarization is known as Circular Dichroism (CD) and this was confirmed in the reflection coefficient of the palm of the hand (Hayut et al., 2014). Experimental verification of circular dichroism was provided at two

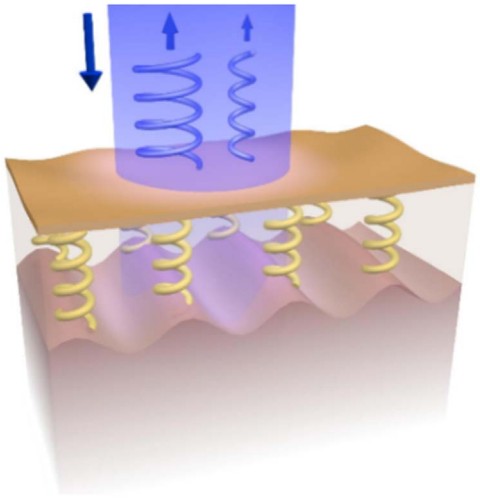

**Fig. 5.** In the schematic above the blue arrows represent the impinging linear wave and reflected circular components (right and left handed) of the reflected wave respectively. As the majority of the sweat ducts are right-handed, the reflected wave exhibits predominantly right handed circular polarization.

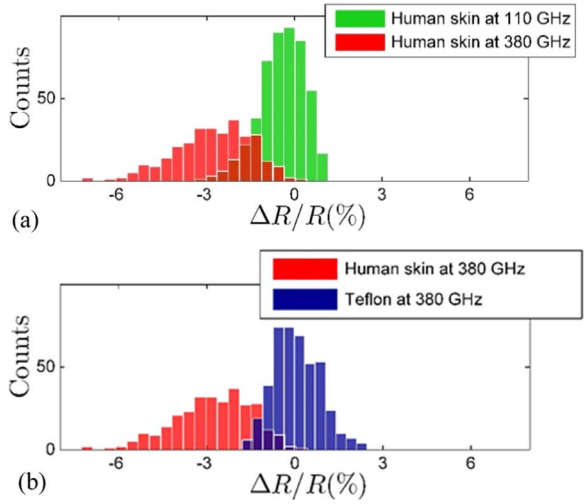


**Fig. 6.** (a) Histograms of the CD measured in the reflection from the skin of one typical human subject at 380 GHz (left histogram) and from the same subject at 110 GHz (right histogram); (b): Histograms of the CD reflection measurements from the skin of one typical subject (left histogram) and from a Teflon plate (right histogram). Significant nonzero circular dichroism is detected in the reflection from the human skin.

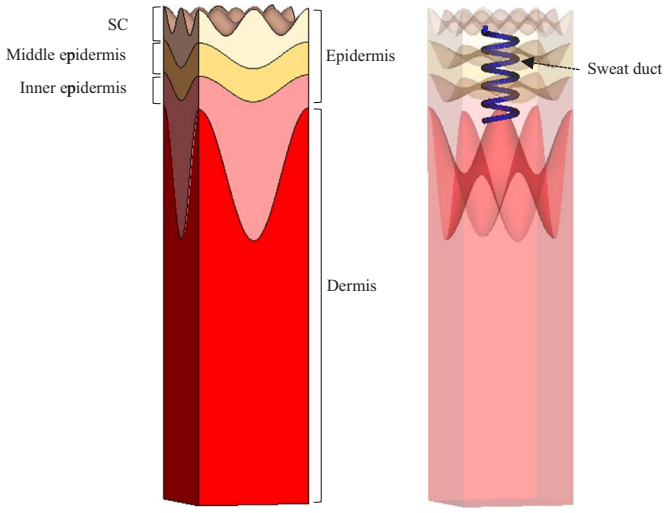


**Fig. 7.** (a)—the model side cross section. The skin is divided into two main layers: dermis and epidermis, where the epidermis layer consists of three sub-layers: SC, middle epidermis (ME), Inner epidermis (IE). (b) — The helical sweat duct located in the epidermis. Sinusoidal functions with different spatial frequencies and amplitudes are used in order to model the non-flat boundaries between the dermis, IE, ME, and SC.

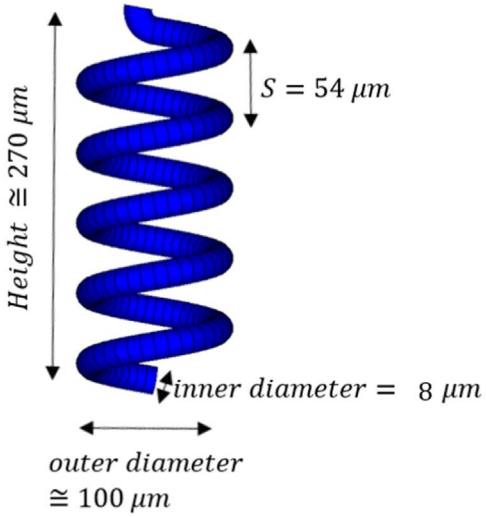


**Fig. 8.** The sweat duct dimensions, which were extracted from optical coherence tomography (OCT) (Tripathi et al., 2015).

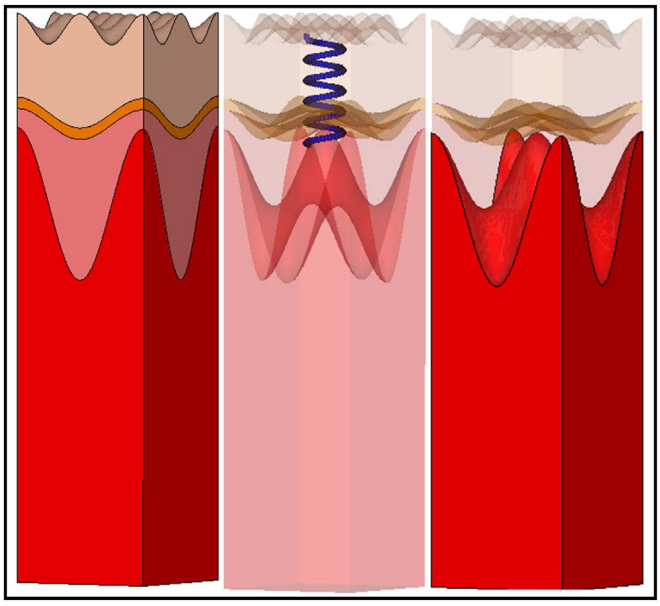

**Fig. 9.** Thick skin. On the left: the model. In the middle: a transparent figure of the model. The helical sweat duct is embedded in the epidermis. On the right - the model with no sweat duct.

frequency points: 380 GHz, which is estimated as the approximate axial mode of the helical structures, and 110 GHz for comparison (only negligible CD is expected at 110 GHz (Hayut et al., 2013)). A typical histogram showing the pronounced CD effect for one subject is presented in Fig. 6. CD was demonstrated at 380 GHz (red histogram) but not at 110 GHz (green histogram - see Fig. 6a). In order to dismiss possible artifacts of the measuring system, CD was also sought for Teflon at 380 GHz, and was not detected. (see Fig. 6b). These results show that the residual CD is not an artefact of the system.

## 4. Computational approach

In the near future, applications will come online that require data transmission in ultra-high rates of 100 Gbit per second and beyond. In fact, the planning for new industry regulations for the exploitation of the sub – THz band are well advanced under the auspices of IEEE 802.15 THz Interest Group (Kürner and Priebe, 2014), and on July 14, 2016, the US Federal Communications Commission (FCC) adopted new rules for wireless broadband operations above 24 GHz (Kürner and Priebe, 2014). In these EHF bands, the dimensions of tissues like skin are on a par with those same wavelengths of the impinging signal. Therefore, the human skin tissues cannot be considered as an infinite layer, compared to the wavelengths of the new communication regulations signal. This reduces the relevance of methods used by the industry today for the assessment of SARs: the use of phantoms (Palka et al., 2013; Reid et al., 2007; Walker et al., 2004) and the alternative electromagnetic simulations software packages. The more sophisticated of these packages are voxel-based models for the Human anatomy (Nagaoka and Watanabe, 2009). Voxel based models were originally developed for the dosimetry of MRI, where the relevant EM wavelengths are in the GHz range. Consequently, for layered structures of less than 1 mm, they are limited (Betzalel et al., 2017). In recent years, the exponentially growing interest in millimeter-wave technologies (Ting Wu et al., 2015a, 2015b), has led to the development of different models and techniques in this field. There are 1-D human tissue models

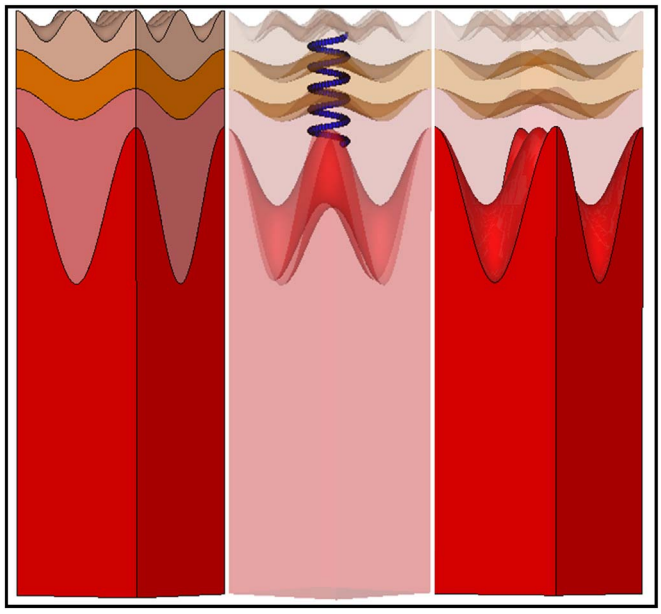

**Fig. 10.** Thin skin. On the left: the model. In the middle: a transparent figure of the model. The helical sweat duct is embedded in the epidermis. On the right - the model with no sweat duct.

representing few typical body parts such as naked skin, naked forehead, clothed skin and forehead (Alekseev and Ziskin, 2007), for the study of heating effects induced by mm Wave exposures on the body; inhomogeneous multilayer skin layer model; unilayer and multilayered models (Chan et al., 2012). Dosimetry of the skin has also been addressed by using multilayered models, coupled with heat perfusion (Sasaki et al., 2017). However, none of these models take into account the helical sweat duct which, as mentioned earlier, plays an important role in shaping the electromagnetic spectral response.

We present a simulation model of the human skin, taking into account its multiple layers, their distinctive water contents and the helical segment of the sweat duct (Betzalel et al., 2017).

Due to the water gradient of the surrounding tissue, the sweat ducts are embedded in a non-uniform medium, i.e. non-uniform conductivity and permittivity. The influence of those water gradients on the axial mode frequency of the duct can be approximated by using an effective permittivity for the medium, according to the formula

$$f_{axial} = \frac{c_0}{2\pi R\sqrt{\varepsilon_{eff}}} \tag{2}$$

$c_0$ is the velocity of light in vacuum, $R$ is the radius of the helical duct and $\varepsilon_{eff} = 5.1$ is an effective dielectric permittivity, derived by a weighted average of all sub layer permittivities (Betzalel et al., 2017; Feldman et al., 2009).

## 5. The model

The model is a unit cell, consisting of two main layers; dermis and epidermis, where the last is divided into three sub-layers: the inner epidermis (IE), the middle epidermis (ME) and the Stratum Corneum (SC) (see Fig. 7). The helical sweat duct was embedded in the epidermis layer since initial studies (Hayut et al., 2013) demonstrate that THz radiation does not penetrate beyond the typical depth of the epidermis layer, i.e. few hundred of micrometers, and therefore the hypodermis does not play an important role in shaping the electromagnetic spectral response. Fig. 8 shows the sweat duct dimensions. The layer dimensions were, SC: 100 μm, ME: 100 μm, IE: 100 μm and Dermis: 1000 μm.

The accuracy of any simulation greatly depends on the boundary conditions as well as on the computational power available. In order to reduce the computational effort and remove boundary effects, an aperiodic boundary condition was applied to the model, so allowing the application of Floquet's theorem for periodic structures (Hayut et al., 2013; Magnus and Winkler, 2004). The emphasis of this research was on SAR values, using point SAR criteria. Although these values can depend on the orientation of the impinging E field, it is enough to consider a perpendicular wave to observe gross tendencies in the frequency dependence of SAR. Therefore, a perpendicular plane wave was selected as the excitation source. In order to check the dependence of the radiation absorption on skin type we simulated SARs for two types of skin models: thin and thick skin, Figs. 9 and 10 respectively. For each type, we changed the ducts' conductivity: 2000, 5000, 10,000 S/m and no duct. The justification for such high values of conductivity can be found in Hayut et al. (Hayut et al., 2013) and is based on measured high rates of diffusion of protons in ordered water layers typically found at lipid/water interfaces. As mentioned earlier, the different

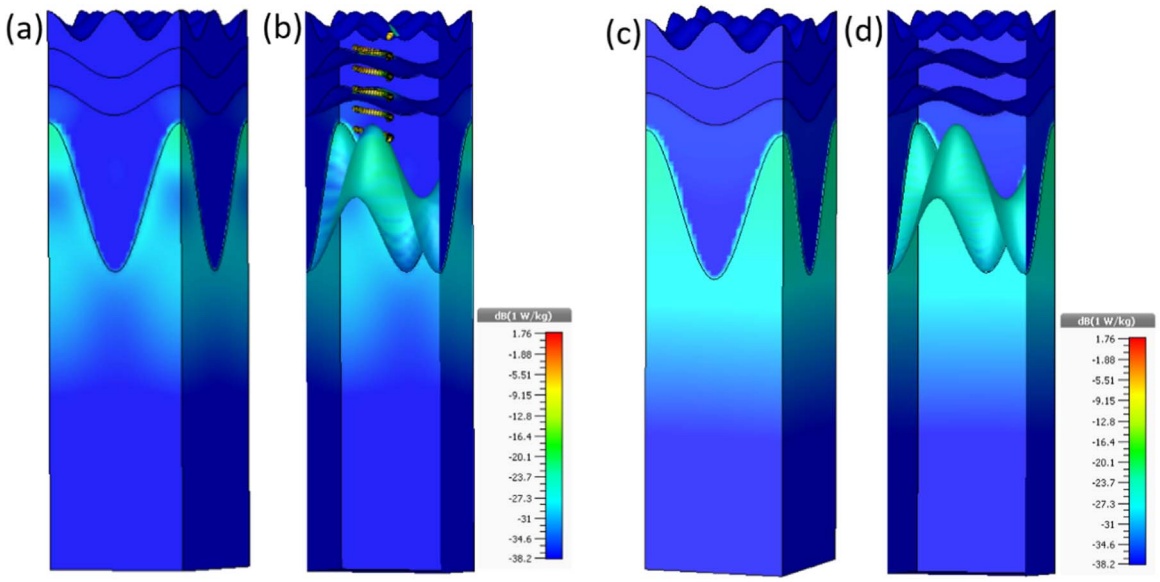


**Fig. 11.** the SARs distribution patterns over the model calculated at a frequency of 440 GHz with a duct ac conductivity of 10,000 S/m, (a) for the thin skin model, (b) the same model showing a cross section exposing the sweat duct, (c) for the thin skin model without an embedded sweat duct and (d) The cross section of the same ductless model. Black indicates a high SAR value (above 1.76 W/kg in dB) and white a low SAR value. The simulation indicates that the main mechanism for sub-THz absorption in the skin layer is via absorption in the duct.

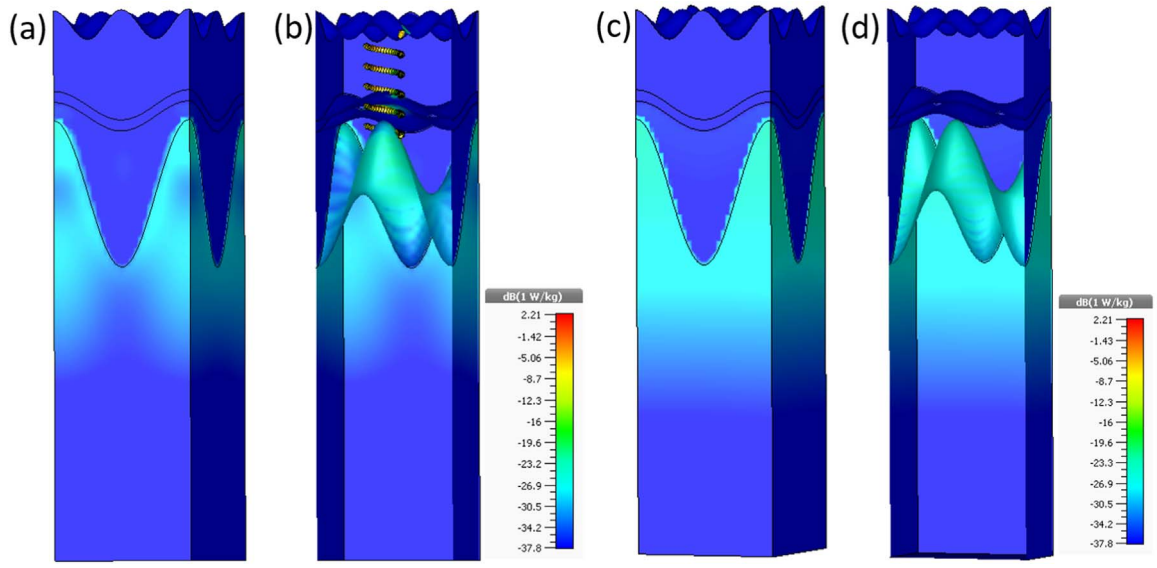


**Fig. 12.** The SAR distribution patterns for the thick skin model calculated at a frequency of 450 GHz and a duct ac conductivity of 10,000 S/m, (a) for the model with an embedded sweat duct, (b) a cross-section of the same model showing the position of the sweat duct, (c) the same model without the presence of a duct and (d) a cross section of the same model. Black indicates a SAR value of above 2.2 W/kg in dB. The results tally with those of the thin skin model, showing the energy is preferentially absorbed in the duct.

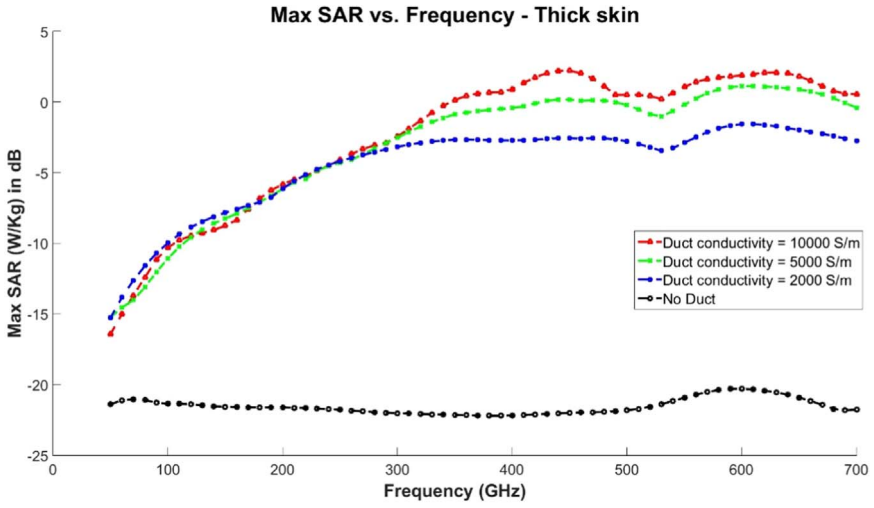


**Fig. 13.** Maximal SAR as a function of the frequency for thick skin.

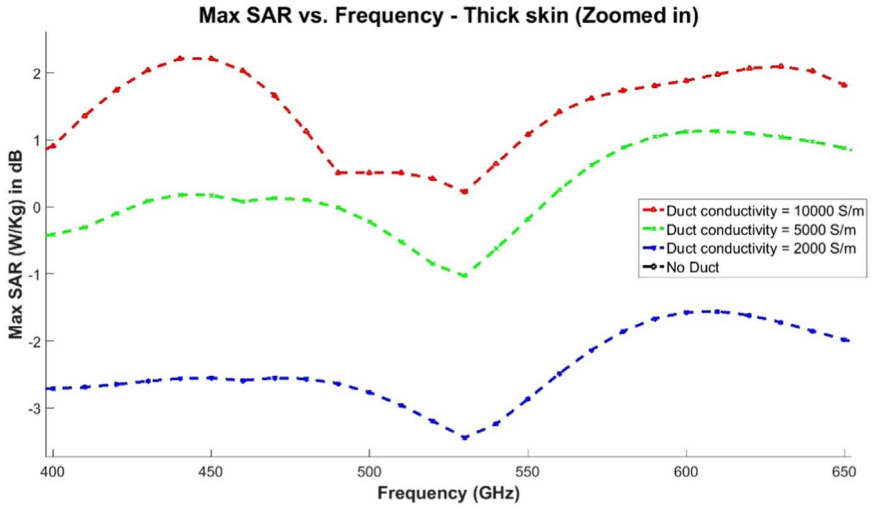


**Fig. 14.** Maximal SAR as a function of the frequency for thick skin. Zoomed-in on frequency range of 400–650 GHz.

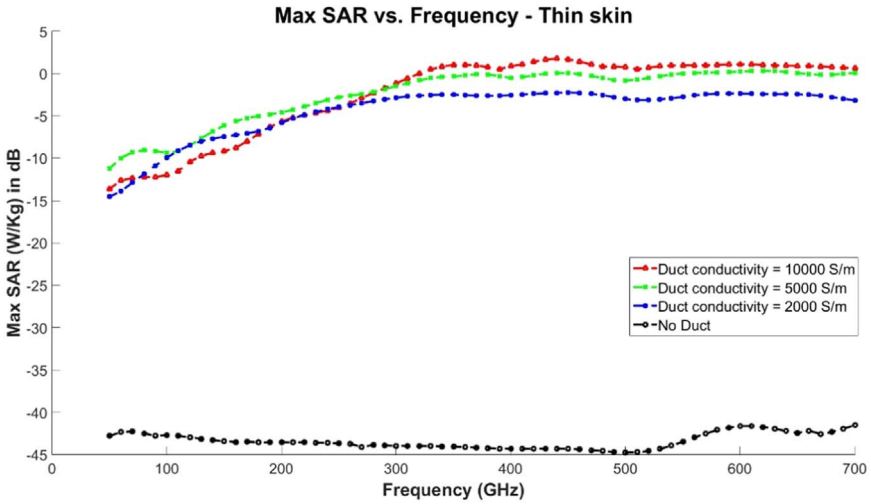


**Fig. 15.** Maximal SAR as a function of the frequency for thin skin.

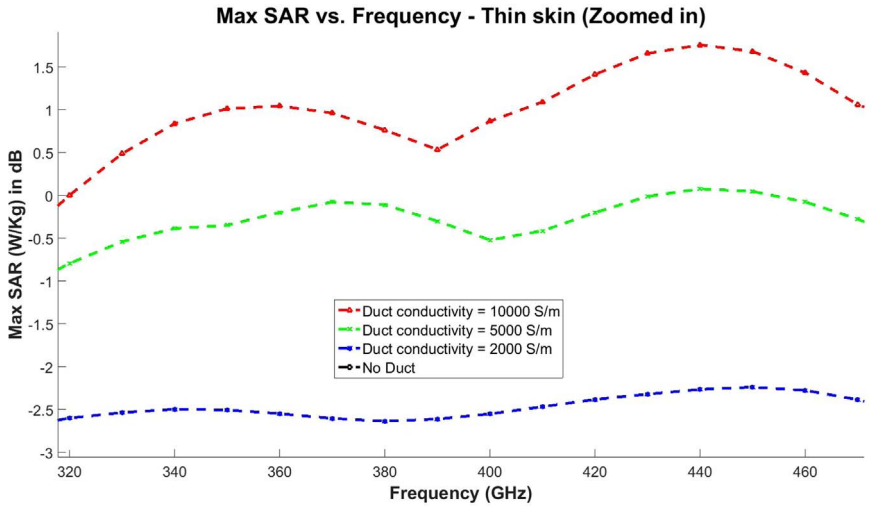


**Fig. 16.** Maximal SAR as a function of the frequency for thin skin. Zoomed-in on frequency range of 320–470 GHz.

conductivities of the sweat duct correspond to different activity level of the sweat gland, i.e. high conductivity corresponds to high activity of the gland (Hayut et al., 2013).

## 6. Results

Fig. 11 displays the SARs distribution patterns over the model calculated at a frequency of 440 GHz. The duct ac conductivity was set to 10,000 S/m, (a) for the thin skin model (Fig. 10), (b) the same model showing a cross section exposing the sweat duct, (c) for the thin skin model without an embedded sweat duct and (d) the cross section of the same ductless model. Black indicates a high SAR value (above 1.76 W/kg in dB) and white a low SAR value. The simulation indicates that the main mechanism for sub-THz absorption in the skin layer is via absorption in the duct. Fig. 12 displays the SAR distribution patterns for the thick skin model. It is calculated at a frequency of 450 GHz with the duct ac conductivity set to 10,000 S/m. Fig. 12(a) for the model with an embedded sweat duct, (b) a cross-section of the same model showing the position of the sweat duct, (c) the same model without the presence of a duct and (d) a cross section of the same model. Black indicates a SAR value of above 2.2 W/kg in dB. The results tally with those of the thin skin model, showing that the energy is preferentially absorbed in the duct.

We calculated the maximal SAR as a function of the frequency for each type of model (thick and thin skin model) as can be seen in Fig. 13 (for thick skin) and Fig. 14 (for thin skin) (Fig. 15)

The optimal frequencies for absorbance by human skin are represented by the peak in the Maximal SAR vs. frequency graphs according to the axial frequency predicted by Eq. (2). The thick skin model exhibit strong peaks at 410 GHz and 500 GHz and the thin skin model exhibits two strong peaks at 440 GHz and 580 GHz. The influence of the ac conductivity of the duct is clearly evident in Fig. 14 (thick skin) and Fig. 16 (thin skin), it is clear that at even low levels of 2000 S/m, the level of SARs is still high in respect to the SAR level obtained for the model without the duct.

Visualizing the Electric field distributions inside the model (Figs. 17and 18) further accentuate these conclusions. The EM field concentrates in the duct where it is effectively absorbed.

## 7. Conclusions

The need for high data transmission rates, coupled with advances in semiconductor technology, is pushing the communications industry towards the sub-THz frequency spectrum. While the promises of a glorious future, resplendent with semi-infinite data streaming, may be attractive, there is a price to pay for such luxury. We shall find our cities, workspace and homes awash with 5 G base stations and we shall live though an unprecedented EM smog. The benefits to our society of

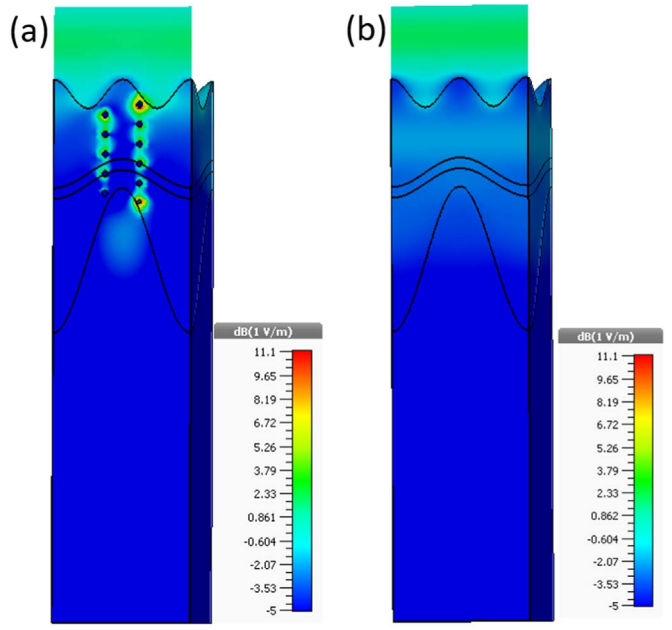


**Fig. 17.** Cross-section of the E-field of a thick skin in frequency of 450 GHz. (a) Model with duct. Red indicates an E-field of value 11.1 V/m in dB (b) Model without duct.

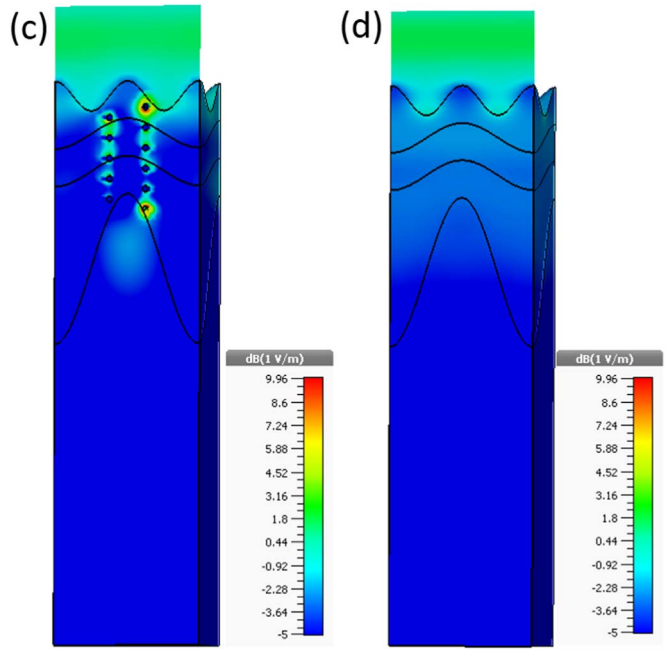


**Fig. 18.** Cross-section of the E-field of a thin skin in frequency of 450 GHz. (c) Model with duct. Red indicates an E-field of value 9.96 V/m in dB (d) Model without duct.

becoming so wired cannot ignore possible health concerns, as yet unexplored. There is enough evidence to suggest that the combination of the helical sweat duct and wavelengths approaching the dimensions of skin layers could lead to non-thermal biological effects. Such fears should be investigated and these concerns should also effect the definition of standards for the application of 5G communications.

## References


Adams, J.A., Galloway, T.S., Mondal, D., Esteves, S.C., Mathews, F., 2014. Effect of mobile telephones on sperm quality: a systematic review and meta-analysis. Environ. Int. 70, 106–112. http://dx.doi.org/10.1016/j.envint.2014.04.015.

Agiwal, M., Roy, A., Saxena, N., 2016. Next Generation 5G Wireless Networks: a Comprehensive Survey. IEEE Commun. Surv. Tutor. 18, 1617–1655. http://dx.doi.org/10.1109/COMST.2016.2532458.

Alekseev, S.I., Ziskin, M.C., 2007. Human skin permittivity determined by millimeter wave reflection measurements. Bioelectromagnetics 28, 331–339. http://dx.doi.org/10.1002/bem.20308.

Ben Ishai, P., Tripathi, R., Kawase, S., Puzenko, K., Feldman, Y, A., 2016. What is the primary mover of water dynamics? Phys. Chem. Chem. Phys. 17, 15428–15434. http://dx.doi.org/10.1039/C5CP01871D.

Betzalel, N., Feldman, Y., Ben Ishai, P., 2017. The Modeling of the Absorbance of Sub-THz Radiation by Human Skin. IEEE Trans. Terahertz Sci. Technol. 1–8. http://dx.doi.org/10.1109/TTHZ.2017.2736345.

Blank, M., Goodman, R., 2009. Electromagnetic fields stress living cells. Pathophysiol., Electromagn. Fields (EMF) Spec. Issue 16, 71–78. http://dx.doi.org/10.1016/j.pathophys.2009.01.006.

Boccardi, F., Heath, R.W., Lozano, A., Marzetta, T.L., Popovski, P., 2014. Five disruptive technology directions for 5G. IEEE Commun. Mag. 52, 74–80. http://dx.doi.org/10.1109/MCOM.2014.6736746.

Brändén, M., Sandén, T., Brzezinski, P., Widengren, J., 2006. Localized proton microcircuits at the biological membrane–water interface. Proc. Natl. Acad. Sci. 103, 19766–19770. http://dx.doi.org/10.1073/pnas.0605909103.

Cacioppo, J.T., Tassinary, L.G., Berntson, G. (Eds.), 2007. Handbook of Psychophysiology, 3rd ed. Cambridge University Press, Cambridge. http://dx.doi.org/10.1017/CBO9780511546396.

Chan, K.H., Leung, S.W., Diao, Y.L., Siu, Y.M., Ng, K.T., 2012. Analysis of millimeter wave radiation to human body using inhomogeneous multilayer skin model, In: 2012 Asia-Pacific Symposium on Electromagnetic Compatibility. Presented at the 2012 Asia-Pacific Symposium on Electromagnetic Compatibility, pp. 721–724. doi:10.1109/APEMC.2012.6237955.

Darbandi, M., Darbandi, S., Agarwal, A., Henkle, R., Sadeghi, M.R., 2017. The Effects of Exposure to Low Frequency Electromagnetic Fields on Male Fertility. Altern. Ther. Health Med.

Eisenach, J.H., Atkinson, J.L.D., Fealey, R.D., 2005. Hyperhidrosis: evolving therapies for a well-established phenomenon. Mayo Clin. Proc. 80, 657–666. http://dx.doi.org/10.4065/80.5.657.

Ellison, W.J., Lamkaouchi, K., Moreau, J.-M., 1996. Water: a dielectric reference. J. Mol. Liq. 68, 171–279. http://dx.doi.org/10.1016/0167-7322(96)00926-9.

Feldman, Y., Puzenko, A., Ben Ishai, P., Caduff, A., Agranat, A.J., 2008. Human Skin as Arrays of Helical Antennas in the Millimeter and Submillimeter Wave Range. Phys. Rev. Lett. 100, 128102. http://dx.doi.org/10.1103/PhysRevLett.100.128102.

Feldman, Y., Puzenko, A., Ishai, P.B., Caduff, A., Davidovich, I., Sakran, F., Agranat, A.J., 2009. The electromagnetic response of human skin in the millimetre and submillimetre wave range. Phys. Med. Biol. 54, 3341. http://dx.doi.org/10.1088/0031-9155/54/11/005.

Gabriel, S., Lau, R.W., Gabriel, C., 1996. The dielectric properties of biological tissues: iii. Parametric models for the dielectric spectrum of tissues. Phys. Med. Biol. 41, 2271–2293.

Ge, X., Tu, S., Mao, G., Wang, C.X., Han, T., 2016. 5G Ultra-Dense Cellular Networks. IEEE Wirel. Commun. 23, 72–79. http://dx.doi.org/10.1109/MWC.2016.7422408.

Guidelines for limiting exposure to time-varying electric, magnetic, and electromagnetic fields (up to 300 GHz). International Commission on Non-Ionizing Radiation Protection Health Phys. 74 1998 494 522.

Guyton, A.C., 1990. Textbook of MedicalPhysiology, 8th ed. Harcourt College Pub, Philadelphia.

Habauzit, D., Le, Q., Zhadobov, M., Martin, C., Aubry, M., Sauleau, R., Le, D., 2014. Transcriptome analysis reveals the contribution of thermal and the specific effects in cellular response to millimeter wave exposure. PLoS ONE 9. http://dx.doi.org/10.1371/journal.pone.0109435.

Hardell, L., Sage, C., 2008. Biological effects from electromagnetic field exposure and public exposure standards. Biomed. Pharmacother. 62, 104–109. http://dx.doi.org/10.1016/j.biopha.2007.12.004.

Hayut, I., Ben Ishai, P., Agranat, A.J., Feldman, Y., 2014. Circular polarization induced by the three-dimensional chiral structure of human sweat ducts. Phys. Rev. E 89, 042715. http://dx.doi.org/10.1103/PhysRevE.89.042715.

Hayut, I., Puzenko, A., Ben Ishai, P., Polsman, A., Agranat, A.J., Feldman, Y., 2013. The Helical Structure of Sweat Ducts: their Influence on the Electromagnetic Reflection Spectrum of the Skin. IEEE Trans. Terahertz Sci. Technol. 3, 207–215. http://dx.doi.org/10.1109/TTHZ.2012.2227476.

Hubbard, B.L., Gibbons, R.J., Lapeyre, A.C., Zinsmeister, A.R., Clements, I.P., 1992. Identification of severe coronary artery disease using simple clinical parameters. Arch. Intern. Med. 152, 309–312.

Kim, J., Lu, W., Qiu, W., Wang, L., Caffrey, M., Zhong, D., 2006. Ultrafast hydration dynamics in the lipidic cubic phase: discrete water structures in nanochannels. J. Phys. Chem. B 110, 21994–22000. http://dx.doi.org/10.1021/jp062806c.

Kirschbaum, C., Pirke, K.M., Hellhammer, D.H., 1993. The'Trier Social Stress Test'–a tool for investigating psychobiological stress responses in a laboratory setting. Neuropsychobiology 28, 76–81 (doi:119004).

Kraus, J.D., Marhefka, R.J., 2001. Antennas, 3rd edition. McGraw-Hill Education, Singapore, Boston, Mass.

Kürner, T., Priebe, S., 2014. Towards THz Communications - Status in Research, Standardization and Regulation. J. Infrared Millim. Terahertz Waves 35, 53–62. http://dx.doi.org/10.1007/s10762-013-0014-3.

Lademann, J., Otberg, N., Richter, H., Meyer, L., Audring, H., Teichmann, A., Thomas, S., Knüttel, A., Sterry, W., 2007. Application of optical non-invasive methods in skin physiology: a comparison of laser scanning microscopy and optical coherent tomography with histological analysis. Skin. Res. Technol. 13, 119–132. http://dx.doi.org/10.1111/j.1600-0846.2007.00208.x.

Le Dréan, Y., Mahamoud, Y.S., Le Page, Y., Habauzit, D., Le Quément, C., Zhadobov, M.,

Sauleau, R., 2013. State of knowledge on biological effects at 40–60 GHz. Comptes Rendus Phys. 14, 402–411. http://dx.doi.org/10.1016/j.crhy.2013.02.005.
Liu, C., Duan, W., Xu, S., Chen, C., He, M., Zhang, L., Yu, Z., Zhou, Z., 2013. Exposure to 1800MHz radiofrequency electromagnetic radiation induces oxidative DNA base damage in a mouse spermatocyte-derived cell line. Toxicol. Lett. 218, 2–9. http://dx.doi.org/10.1016/j.toxlet.2013.01.003.
Magnus, W., Winkler, S., 2004. Hill's Equation. Dover Publications, Mineola, N.Y.
Mahamoud, Y.S., Aite, M., Martin, C., Zhadobov, M., Sauleau, R., Dréan, Y.L., Habauzit, D., 2016. Additive Effects of Millimeter Waves and 2-Deoxyglucose Co-Exposure on the Human Keratinocyte Transcriptome. PLOS ONE 11, e0160810. http://dx.doi.org/10.1371/journal.pone.0160810.
Muter, P., Furedy, J.J., Vincent, A., Pelcowitz, T., 1993. User-hostile systems and patterns of psychophysiological activity. Comput. Hum. Behav. 9, 105–111. http://dx.doi.org/10.1016/0747-5632(93)90025-N.
Nagaoka, T., Watanabe, S., 2009. Voxel-based variable posture models of human anatomy. Proc. IEEE 97, 2015–2025. http://dx.doi.org/10.1109/JPROC.2009.2025662.
Nishiyama, T., Sugenoya, J., Matsumoto, T., Iwase, S., Mano, T., 2001. Irregular activation of individual sweat glands in human sole observed by a videomicroscopy. Auton. Neurosci. 88, 117–126. http://dx.doi.org/10.1016/S1566-0702(01)00229-6.
Ohhashi, T., Sakaguchi, M., Tsuda, T., 1998. Human perspiration measurement. Physiol. Meas. 19, 449–461. http://dx.doi.org/10.1088/0967-3334/19/4/001.
Palka, N., Ryniec, R., Piszczek, M., Kowalski, M., Rurka, E., Szustakowski, M., 2013. Construction and evaluation of the terahertz human phantom. Przegląd Elektrotech. R. 89.
Panagopoulos, D.J., 2017. Mobile Telephony EMFs Effects on Insect Ovarian Cells. The Necessity for Real Exposures Bioactivity Assessment. The Key Role of Polarization, and the "Ion Forced-Oscillation Mechanism,". In: Microwave Effects on DNA and Proteins. Springer, Cham, pp. 1–48. http://dx.doi.org/10.1007/978-3-319-50289-2_1.
Popov, I., Ben Ishai, P., Khamzin, A., Feldman, Y., 2016. The mechanism of the dielectric relaxation in water. Phys. Chem. Chem. Phys. 18, 13941–13953. http://dx.doi.org/10.1039/C6CP02195F.
Reid, C., Gibson, A.P., Hebden, J.C., Wallace, V.P., 2007. The use of tissue mimicking phantoms in analysing contrast in THz pulsed imaging of biological tissue, In: 2007 Joint Proceedings of the 32nd International Conference on Infrared and Millimeter Waves and the 15th International Conference on Terahertz Electronics. Presented at the 2007 Joint 32nd International Conference on Infrared and Millimeter Waves and the 15th International Conference on Terahertz Electronics, pp. 567–568. doi:10.1109/ICIMW.2007.4516632.
Safrai, E., Ben Ishai, P., Polsman, A., Einav, S., Feldman, Y., 2014. The Correlation of ECG Parameters to the Sub-THz Reflection Coefficient of Human Skin. IEEE Trans. Terahertz Sci. Technol. 4, 624–630. http://dx.doi.org/10.1109/TTHZ.2014.2342499.
Safrai, E., Ishai, P.B., Caduff, A., Puzenko, A., Polsman, A., Agranat, A.J., Feldman, Y., 2012. The remote sensing of mental stress from the electromagnetic reflection coefficient of human skin in the sub-THz range. Bioelectromagnetics 33, 375–382. http://dx.doi.org/10.1002/bem.21698.
Sage, C., Carpenter, D.O., 2009. Public health implications of wireless technologies. Pathophysiol., Electromagn. Fields (EMF) Spec. Issue 16, 233–246. http://dx.doi.org/10.1016/j.pathophys.2009.01.011.
Sasaki, K., Mizuno, M., Wake, K., Watanabe, S., 2017. Monte Carlo simulations of skin exposure to electromagnetic field from 10 GHz to 1 THz. Phys. Med. Biol. 62, 6993–7010. http://dx.doi.org/10.1088/1361-6560/aa81fc.
Serup, J., Trier-Mork, T., 2007. Taking Skin Research & Technology another step forward. Skin. Res. Technol. 13 (1–1). http://dx.doi.org/10.1111/j.1600-0846.2007.00234.x.
Stroop, J.R., 1935. Studies of Interference in Serial Verbal Reactions. J. Exp. Psychol. 18, 643.
Terzi, M., Ozberk, B., Deniz, O.G., Kaplan, S., 2016. The role of electromagnetic fields in neurological disorders. J. Chem. Neuroanat., Controv. Electromagn. Fields Neurobiol. Org. 75, 77–84. http://dx.doi.org/10.1016/j.jchemneu.2016.04.003.
Walker, G.C., Berry, E., Smye, S.W., Brettle, D.S., 2004. Materials for phantoms for terahertz pulsed imaging. Phys. Med. Biol. 49, N363–N369.
Wu, T., Rappaport, T.S., Collins, C.M., 2015a. Safe for Generations to Come: considerations of Safety for Millimeter Waves in Wireless Communications. IEEE Microw. Mag. 16, 65–84. http://dx.doi.org/10.1109/MMM.2014.2377587.
Wu, T., Rappaport, T.S., Collins, C.M., 2015b. Human. Body Millim.-Wave Wirel. Commun. Syst.: Interact. Implic (ArXiv150305944 Cs).
Zhadobov, M., Chahat, N., Sauleau, R., Quement, C.L., Drean, Y.L., 2011. Millimeter-wave interactions with the human body: state of knowledge and recent advances. Int. J. Microw. Wirel. Technol. 3, 237–247. http://dx.doi.org/10.1017/S1759078711000122.
Ziegler, H., Heidl, M., 2008. Biomimetic Tripeptides for Improved dermal transport. Cosmet. Toilet. 122, 59–67.

## Further reading

Benisha, M., Prabu, R.T., Bai, V.T., 2016. Requirements and challenges of 5G cellular systems, In: 2016 Proceedings of the 2nd International Conference on Advances in Electrical, Electronics, Information, Communication and Bio-Informatics (AEEICB). Presented at the 2016 2nd InternationalConference on Advances in Electrical, Electronics, Information, Communication and Bio-Informatics (AEEICB), pp. 251–254. doi:10.1109/AEEICB.2016.7538283.